Research Article Vol. 62, No. 7 / 1 March 2023 / Applied Optics B35

applied optics

Reverse engineering of e-beam deposited optical filters based on multi-sample photometric and ellipsometric data

Tatiana Amotchkina,[1,*] Michael Trubetskov,[1,2] Vesna Janicki,[3] and Jordi Sancho-Parramon[3]

[1]Optilayer GmbH, Carl-Zeiss-Ring 11-17, 85737 Ismaning, Germany
[2]Max-Planck Institute of Quantum Optics, Hans-Kopfermann Str. 1, 85748 Garching, Germany
[3]Ruđer Bošković Institute, Bijenička cesta 54, 10002 Zagreb, Croatia
*Corresponding author: amotchkina@optilayer.com

Received 30 September 2022; revised 11 November 2022; accepted 15 November 2022; posted 17 November 2022; published 13 December 2022

A post-production characterization approach based on spectral photometric and ellipsometric data related to a specially prepared set of samples is proposed. Single-layer (SL) and multilayer (ML) sets of samples presenting building blocks of the final sample were measured *ex-situ*, and reliable thicknesses and refractive indices of the final ML were determined. Different characterization strategies based on *ex-situ* measurements of the final ML sample were tried, reliability of their results was compared, and the best characterization approach for practical use, when preparation of the mentioned set of samples would be a luxury, is proposed.

https://doi.org/10.1364/AO.477181

1. INTRODUCTION

Characterization of e-beam deposited TiO_2/SiO_2 coatings is not a straightforward task. It is known that the refractive indices of evaporated TiO_2 layers are dependent on deposition conditions [1,2]; in additions, may vary from layer to layer [1]. It may also happen that the *nominal* refractive indices, i.e., the refractive indices used in the process of theoretical designing, may differ from the *actual* refractive indices of coating layers [3]. Very often, nominal refractive indices determined based on characterization of thick single layers may be slightly different from the optical constants of coating layers, which are usually thinner.

A series of papers reporting various aspects of post-production characterization of multilayer (ML) coatings has been published. In [4], quarter-wave mirrors were characterized on the basis of multi-scan transmittance measurements recorded by a broadband monitoring (BBM) device [5]. The coatings were produced using magnetron sputtering, and layer thicknesses were controlled by very accurate time monitoring. During the deposition, the errors were induced on some layer thicknesses that allowed considering this characterization problem as an *academic example*, i.e., a problem with a known result. Knowing the layer errors with good accuracy allowed one to compare triangular and sequential characterization algorithms [6] and to prove that a triangular algorithm provides more reliable results, at least in the case of BBM data.

In [7], similar quarter-wave mirrors with known induced errors in some layer thicknesses were used to select a dataset providing reliable characterization results. It was demonstrated that *ex-situ* reflectance/transmittance (R/T) measurements, including informative features (characteristic minima and maxima, noticeable variations of the curves) in the short wavelength spectral range, can be considered as a basis for reliable post-production characterization.

In [8], complex oblique incidence coatings were carefully characterized, namely, a 28-layer edge filter deposited by ion-assisted deposition, a 52-layer beam splitter deposited by magnetron sputtering, and a 43-layer quarter-wave mirror produced by e-beam evaporation. The layer thicknesses were controlled by three different monitoring methods: BBM, time monitoring, and quartz crystal monitoring, respectively. The parameters of the coatings were estimated based on normal incidence BBM transmittance scans and *ex-situ* normal incidence spectral photometric measurements. Characterization results were validated with the help of multi-angular measurements [9].

In works [4,7,8], mainly coatings with dense layers and stable refractive indices were investigated. In such a case, it might be expected that characterization results obtained from *in-situ* BBM data and *ex-situ* R/T measurements are identical or very similar. In the case of e-beam deposited coatings, layer parameters obtained based on BBM data can be considered as a starting approximation of the actual coating parameters only. Since the microstructure of the films deposited by an evaporation

technique may change after exposition to the atmosphere due to the absorption of humidity, their optical constants may change as well. This phenomenon is well known as vacuum shift (see, for example, [10]). The layer thicknesses may also have slight changes due to the "swelling" of the layers. In [8], in order to simplify the coatings model, it was assumed that the layer thicknesses do not change, and the refractive indices of all high index layers vary at the same value.

E-beam evaporation is an industrially well-established thin film technique due to the high deposition rates of the layers, large area uniformity of the coatings, and wide choice of materials that can be used. The porosity in the layers can be minimized by careful optimization of deposition conditions, or it can be taken into account during design and characterization of the coatings.

Post-production characterization of e-beam deposited coatings is a complicated task, even if researchers have BBM scans at their disposal. As mentioned before. the optical properties of coatings differ in vacuum and after exposition to the atmosphere because the layers absorb water from air, and their structures change. BBM data are related to the coating in vacuum and, therefore, by analyzing this data with the help of a triangular algorithm, it is possible to obtain estimations of errors in layer thicknesses only. The final determination of the layer parameters of the produced coatings can be done on the basis of *ex-situ* spectral photometric and/or ellipsometric data. The errors in the layer thicknesses obtained from BBM characterization are to be considered as good approximations for actual errors. This means that if the errors determined from *ex-situ* R/T or ellipsometric data differ essentially from the ones obtained from BBM data; then these errors and layer optical constants cannot be considered as reliable ones.

It should be noted that *not all deposition plants are equipped with BBM devices*. At the same time, careful characterization of e-beam deposited coatings is required. This problem is especially important if new materials are introduced or modifications of the deposition plant that affect the conditions of evaporation were made (new equipment, cleaning, etc.). In the present study, a unique set of e-beam deposited coatings was produced, and a series of spectral photometric and ellipsometric measurements related to these samples was performed. Based on the experimental data, the produced samples were carefully characterized. In the process of characterization, the following questions were answered:

- Which minimum experimental dataset is enough for the reliable characterization of e-beam deposited coatings?
- Which coating model describes such coatings with sufficient accuracy?
- Which numerical algorithm provides reliable post-production characterization results?

A new post-production characterization approach has been applied to find a numerical algorithm providing reliable values of the final multilayer, which practical, even when only one set of *ex-situ* measurements of the complete coating is available. Thus, the presented approach enabled finding a combination of a coating model and the corresponding numerical algorithm providing reliable results. The approach is highly appropriate in the typical cases when *in-situ* BBM scans are not available. The approach steps include:

- Production of a test set of single-layer and multilayer samples.
- Characterization of single layers.
- Characterization of multilayer samples with the help of various combinations of *coating model* and *algorithm*, and verification of the results. The selection of a numerical algorithm that, using one set of measurements of a final multilayer only, results in the most reliable coating model.

2. EXPERIMENTAL SAMPLES AND MEASUREMENT DATA

For the present study, an 11-layer coating with theoretical transmittance plotted in Fig. 1 was chosen. The coating was supposed to have high transmittance in the spectral range from 515 to 545 nm and low transmittance in the range from 1000 to 1100 nm. The choice of the design structure does not play an important role in this study. (1) The chosen design contains an average number of layers; (2) the spectral characteristics of the design after the deposition of each new layer contain many informative features; (3) the design does not contain ultrathin layers; (4) the chosen layer thicknesses are typical for a visible-near-infrared spectral range. The coating was designed for a TiO_2/SiO_2 material pair and BK7 substrate of 1 mm thickness. Nominal optical constants of the high and low index materials, $n_H(\lambda)$, $k_H(\lambda)$ and $n_L(\lambda)$, as well as a refractive index of the BK7 substrate, are described by Cauchy and exponential formulas, respectively [wavelength λ is given in microns in Eq. (1)]:

$$n(\lambda) = A_0 + A_1\lambda^{-2} + A_2\lambda^{-4},$$

$$k(\lambda) = B_0 \exp\left\{B_1\lambda^{-1} + B_2\lambda\right\}. \quad \textbf{(1)}$$

In Eq. (1), $A_0 = 2.154648$, $A_1 = 0.02567$, $A_2 = 0.00449$, $B_0 = 1.1394 \cdot 10^5$, $B_1 = -1.446876$, $B_2 - 35.415620$ for TiO_2, $A_0 = 1.447$, $A_1 = 0.00313$, $A_2 = 4.3353 \cdot 10^{-5}$ for

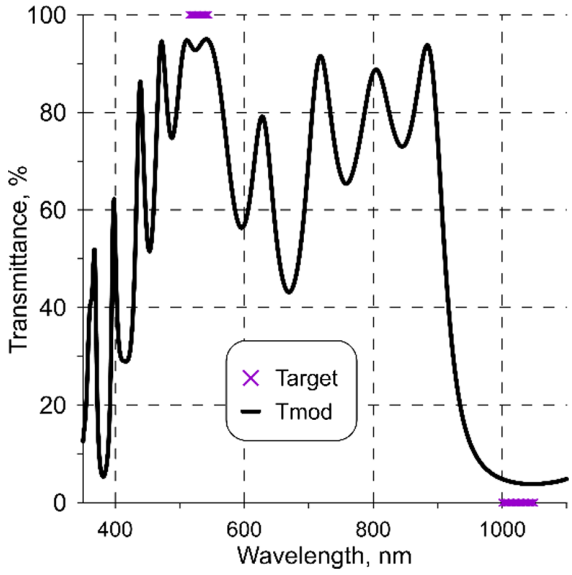

Fig. 1. Model and target transmittance of the 11-layer design.

SiO_2 and $A_0 = 1.503538$, $A_1 = 0.005213$, $A_2 - 9.06137 \cdot 10^{-5}$ for BK7. The nominal refractive index values at the wavelength of 600 nm are 2.262 (TiO2), 1.458 (SiO2), and 1.517 (BK7); the extinction coefficient (TiO2) is $2.58 \cdot 10^{-7}$. The extinction coefficients of SiO_2 and BK7 were set to zero, since the absorption is negligible in the spectral range of interest from 350 to 1100 nm. The refractive indices of many typical thin film materials operate in the visible-near-infrared spectral ranges. The approach suggested in this work can be applied for other dispersion models, for example, the Sellmeier model, or more complex models described by a larger number of parameters.

The theoretical thicknesses $d_1, \ldots, d_{11}$ of coating layers are 100.3, 154.9, 132.5, 187.6, 122.9, 179.7, 125.7, 163.4, 86.6, 255.3, and 112.3 nm; the layers are numbered starting from the substrate, the first layer is the TiO_2 layer.

The samples were produced by an electron beam evaporation technique. The layers were deposited onto substrates pre-heated to 230°C positioned at rotating calotte. The base pressure was $5 \cdot 10^{-6}$ Torr, and the O_2 partial pressure during the deposition of TiO_2 was $9 \cdot 10^{-5}$ Torr. The deposition rates were 10 /s for both SiO_2 and TiO_2 materials. The mass thickness of the layers was controlled by the quartz crystal monitor. All the layers of the same thickness were prepared in the same run. Since the goal was to get the optical measurements of the multilayer at all steps of the fabrication, as with the single material coating, the chamber had to be opened and the corresponding samples had to be taken out after the deposition of each successive layer.

Therefore, the schematic of our experiment was as follows. First, 11 uncoated BK7 substrates were put into the deposition plant. After the deposition of the first layer, the sample number 1 (SL1 = ML1) was taken out, and a new bare substrate for the next single material coating was added into the chamber. After the deposition of the second layer, another single layer (SL2) and the first multilayer sample (ML2) were finished. Each layer followed the same procedure. Schematic of the experimental samples is shown in Fig. 2. As the result, 21 experimental samples were produced, among them:

- Six single-layer samples of TiO_2, denoted as SL_1, SL_3, …, SL_{11}; planned layer thicknesses $d_1, d_3, \ldots, d_{11}$, respectively;
- Five single-layer samples of SiO_2, denoted as SL_2, SL_4, …, SL_{10}; planned thicknesses $d_2, d_4, \ldots, d_{10}$, respectively;
- Ten multilayer coatings containing 2, 3, 4, …, 11 layers and denoted as ML_2, …, ML_{11}.

Two sets of experimental data were collected for each sample: spectrophotometric measurements of transmittance (T) and reflectance (R) under normal incidence (Fig. 3). The reflection was measured using a Perkin–Elmer relative specular reflectance attachment and calibrated reference mirror. The spectrometric measurements of ellipsometric functions (Ψ and Δ) were performed with angles of incidence 45°, 55°, and 65°. Spectrophotometry was performed with Perkin–Elmer Lambda 25, and ellipsometry was performed with a J.A. Woollam V-VASE ellipsometer. The measurements for all samples were made one week after their exposure to the atmosphere. Each of the design layers d_i was also deposited as one of the SL samples and in $(12 - i)$ ML samples $ML_i, \ldots, ML_{11}$. In an ideal case, the layers d_i in the SL and ML samples would be expected to

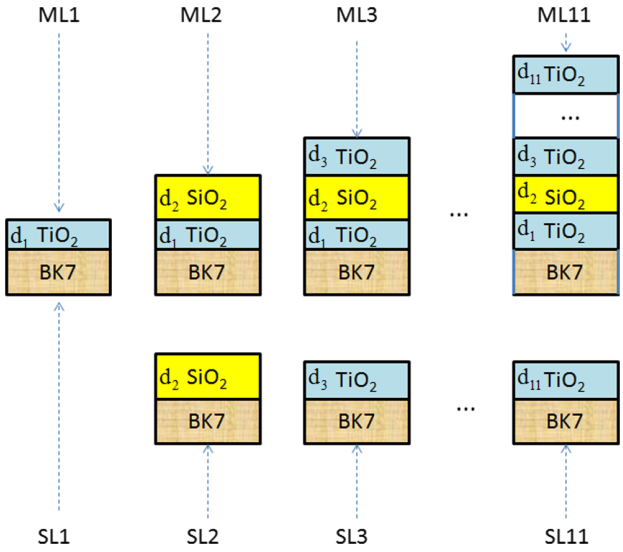

Fig. 2. Schematic of the experimental samples.

be identical. In reality, of course, this is not possible. Due to the experimental conditions, one cannot expect that the optical parameters of the layers in the SL and ML samples are identical. SL samples remained in the atmosphere after a single run, while the ML samples were exposed several times to the environmental conditions and then vacuum before their completing. Due to this procedure, the dynamics of the water absorption process is different in the SL and ML samples and might result in a slight difference in optical properties of the layers. Besides, SLs were grown on bare substrates, while MLs were grown at previously deposited film that may result in different growths and structures of successive layers. Characterization was performed independently based on either spectrophotometric measurements or ellipsometric measurements; the datasets were never combined.

Another reason for deviations between the layer parameters in the SL and ML samples might be the microstructure of the underlying film propagating into the following film; in addition, different material growth on a bare substrate or pre-deposited layer is possible [11].

At the same time, one can expect that the corresponding layer thicknesses in the SL and ML samples are close. This reasoning allows consideration of the characterization of the produced samples as an *academic example*. The characterization results related to the ML samples can be verified by comparing them with the results found in the course of the SL characterization. The layer thicknesses obtained from the characterization process of the SL can be considered as the actual thicknesses $d_1, \ldots, d_i, \ldots, d_{11}$ with sufficient accuracy. Refractive indices of layers in the ML may slightly differ from the ones obtained in the course of the characterization of the SL samples but abrupt variations are not realistic.

It should be noted here that, to the best of our knowledge, this is the first time that such an experimental dataset has been studied. For characterization purposes, OptiLayer Thin Film software [12] was used.

To estimate the closeness between experimental and model coating characteristics, discrepancy functions (DFs) DF_{RT} and DF_{ell} were introduced:

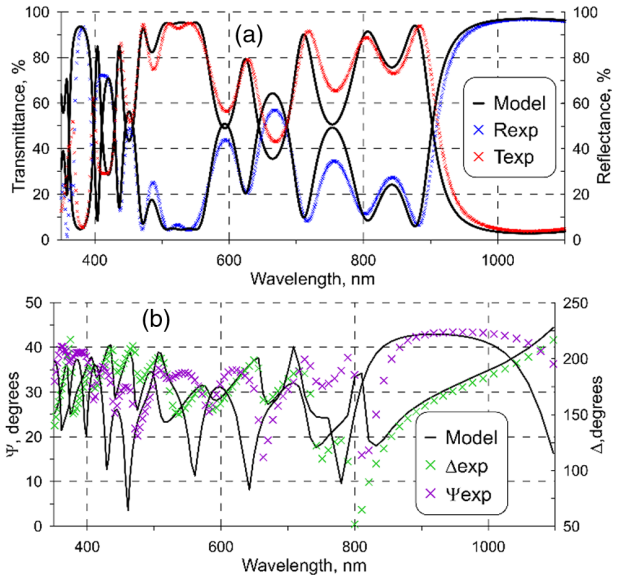

Fig. 3. Comparison of the model design spectral characteristics of 11-layer coating and experimental measurements of the produced sample ML11 (initial comparison): (a) spectrophotometric data R, T; (b) ellipsometric data at AOI = 45°.

$$\mathrm{DF}_{\mathrm{RT}}^2 = \frac{1}{L}\sum_{j=1}^{L}\left\{\left[T(X;\lambda_j) - \hat{T}(\lambda_j)\right]^2 + \left[R(X;\lambda_j) - \hat{R}(\lambda_j)\right]^2\right\}, \quad (2)$$

$$\mathrm{DF}_{\mathrm{ell}}^2 = \frac{1}{L}\sum_{j=1}^{L}\sum_{q=1}^{3}\left[\frac{\Psi(X;\theta_q;\lambda_j) - \hat{\Psi}(\theta_q;\lambda_j)}{\mu_j}\right]^2 + \frac{1}{L}\sum_{j=1}^{L}\sum_{q=1}^{3}\left[\frac{\Delta(X;\theta_q;\lambda_j) - \hat{\Delta}(\theta_q;\lambda_j)}{\nu_j}\right]^2 + \frac{1}{L}\sum_{j=1}^{L}\sum_{q=1}^{3}\left[\frac{\xi(X;\theta_q;\lambda_j) - \hat{\xi}(\theta_q;\lambda_j)}{\chi_j}\right]^2, \quad (3)$$

in the cases of photometric [Eq. (2)] and ellipsometric [Eq. (3)] data. The angles of incidence $\theta_1 = 45^0, \theta_2 = 55^0, \theta_3 = 65^0$; $\hat{T}(\lambda_j)$, $\hat{R}(\lambda_j)$, $\hat{\Psi}(\theta_q;\lambda_j)$, $\hat{\Delta}(\theta_q;\lambda_j)$, $\hat{\xi}(\theta_q;\lambda_j)$ are measured transmittance, reflectance, ellipsometric angles, and the depolarization factor, respectively; μ_j, ν_j, χ_j are experimental uncertainties measured by a Woollam ellipsometer. The measurement data are related to the sample M_{11}. In the following, X is the vector of the model parameters describing optical coating. Initially, $X = \{d_1, \ldots, d_{11}; n_H, n_L, k_H\}$, where $\{d_i\}$ are the theoretical thicknesses of layers, and $\{n_{H,L}, k_H\}$ are nominal refractive indices and extinction coefficients. The initial $\mathrm{DF_{RT}}$ and $\mathrm{DF_{ell}}$ values are equal to 9.3 and 133.2, respectively (Table 1). The theoretical and experimental data related to the $\mathrm{ML_{11}}$ sample are compared in Fig. 1. The deviations between the theoretical and experimental data demonstrate the presence of errors in layer parameters.

Table 1. DF and GDF Values Achieved by Different Characterization Algorithms

Algorithm	Discrepancy		General Discrepancy	
Fitting	DF_{RT}	$\mathrm{DF_{ell}}$	GDF_{RT}	$\mathrm{GDF_{ell}}$
Initial comparison	9.3	133.2	8.7	165.0
SL characterization	2.9	62.0	2.6	63.6
Multi-sample$(n-d)$ algorithm	2.9	83.1	3.6	78.9
Multi-sample $(d-n)$ algorithm	3.6	66.4	2.9	55.18
Multi-sample one-step algorithm	3.5	59.7	3.3	46.8
RE (multiple offsets)	3.6	54.5	3.2	68.9
RE (two-component)	3.4	73.1	3.1	86.3

3. CHARACTERIZATION OF SINGLE LAYERS

In the case of R/T measurements, it was assumed that the refractive index and extinction coefficient wavelength dependencies of TiO_2 are described by Cauchy and exponential models [Eq. (1)], respectively. The refractive indices of SiO_2 layers were described by the Cauchy model; the extinction coefficient was equal to zero. The refractive indices of TiO_2 and SiO_2 layers in SL_1, SL_2 …, SL_{11} samples obtained from spectrophotometric and ellipsometric measurements are shown in Fig. 4; the refractive index values at 600 nm estimated from R/T and the ellipsometric data are compared in Fig. 5; the errors in the layer thicknesses are compared in Fig. 6.

In the case of ellipsometric measurements, absorption in TiO_2 layers was not considered because Ψ, Δ ellipsometric

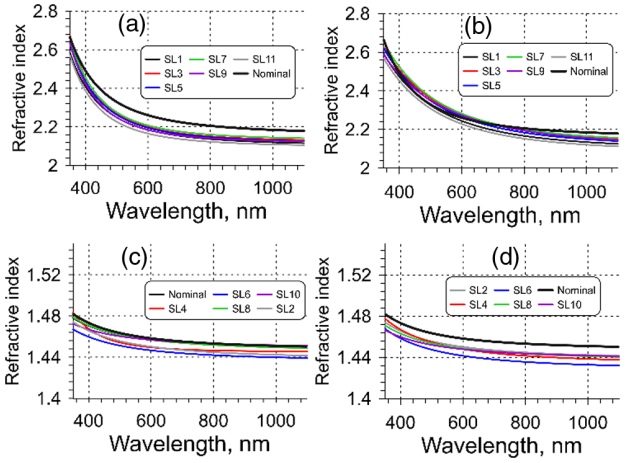

Fig. 4. Wavelength dependencies of (a), (b) TiO_2 and (c), (d) SiO_2 refractive indices obtained from (a), (c) R/T and (b), (d) ellipsometric measurements related to SL samples.

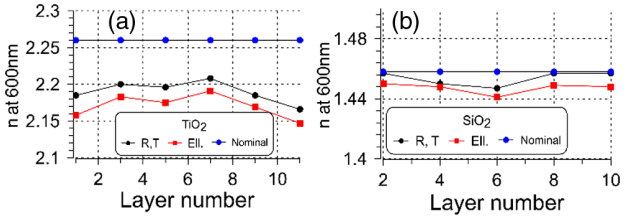

Fig. 5. Comparison of (a) TiO_2 and (b) SiO_2 refractive index values at 600 nm determined from R, T and ellipsometric measurements. The blue markers indicate nominal values.

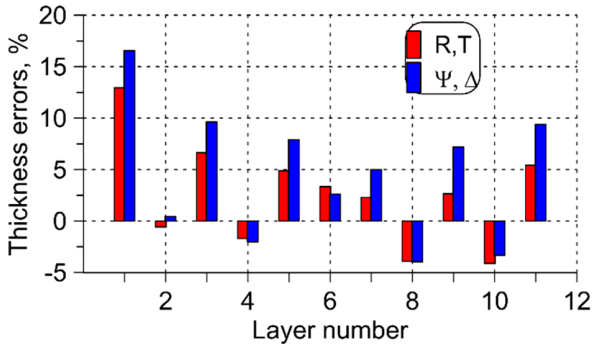

Fig. 6. Relative thickness errors determined during characterization of SL samples on the basis of R, T and ellipsometric data.

angles are almost insensitive to absorption. Even more, introduction of absorption in a thin film model might lead to wrong characterization results in the case of ellipsometry. In the case of ellipsometric measurements, surface roughness of all single TiO_2 layers was estimated. The thicknesses of the overlayers are 2.3 (SL1), 1.5 (SL3), 1.4 (SL5), 1.6 (SL7), 3.2 (SL9), and 2.8 nm (SL11).

It is seen from Fig. 6 that the differences in determined errors in the layer thicknesses in the case of photometric and ellipsometric measurements are small. The maximum deviation does not exceed 2.2% of the planned thickness, which is even less than the similar deviations obtained by the authors of [13]. The refractive index values determined from the ellipsometric data are slightly lower than the ones obtained from the R, T data (see Fig. 5); the deviations do not exceed 0.028, which is the same level as that obtained by the authors of [13]. One reason for these deviations is that ellipsometry is very sensitive to surface roughness, which was not included in the models [14]. TiO_2 films, produced by e-beam evaporation, are typically polycrystalline and should have some roughness, so the refractive index of the film obtained from the model based on ellipsometry data is lower than it would be in the case of the refractive index of an amorphous dense film, as spectrophotometric measurements "see" it. Another explanation is that during the characterization process based on the ellipsometric data, absorption was neglected and was compensated for by a lower refractive index. However, it should not have strong weight, as it affects only the short wavelength part of the spectra. Similarly, the ellipsometry-obtained SiO_2 refractive index is lower as well but, in this case, no absorption is expected. At the same time, it can be observed in Fig. 4 that the refractive index patterns (variations from sample to sample) are similar for both sets of measurement data.

To understand the TiO_2 film structure deeper, packing densities p of the TiO_2 layers were estimated using Bruggemann's formula:

$$n = \frac{1}{2}\sqrt{\rho}, \quad \rho = (3p-1)n_b^2 + (2-3p)n_v^2 + \sqrt{((3p-1)n_b^2 + (2-3p)n_v^2)^2 + 8n_v^2 n_b^2}, \tag{4}$$

where n_b and n_v are the refractive indices of bulk material and water, respectively. The refractive index of the dense TiO_2 film of an ion-beam sputtered process was taken as n_b [15]. The packing densities can be estimated as 78–80%. Assuming that the pores are filled not by water but by air, or a mixture of water and air, there will be similar results: the packing densities differ by 2–3% only. This is correlated with the densities of TiO_2 films produced by e-beam evaporation at the SyrusPro710 deposition plant from Bühler Leybold Optics and reported in our previous work [1].

4. MULTI-SAMPLE CHARACTERIZATION

In Fig. 7, the experimental data related to the ML11 sample (11-layer coating) and its model data are compared. The model data are calculated with the assumption that the multilayer consists of layers with thicknesses and optical constants obtained as the results of SL sample characterization. The DF values were calculated to be equal to 2.9 and 62.0 (see Table 1). In Eqs. (2) and (3), $X = (d_1, \ldots, d_{11}; n_1, \ldots, n_{11})$, where $\{d_i\}$ and $\{n_i\}$ are taken from the results of SL characterization process.

A generalized multi-sample algorithm can be applied to estimation of the optical parameters of the produced samples ML1, …, ML11. Multi-sample measurements related to MLi samples can be considered as analogs of BBM measurement scans recorded after the deposition of the ith layer. The difference is that multi-sample measurements were recorded *ex-situ* seven days after exposing to the atmosphere, in order to allow the vacuum shift to reach its final state. Essential advantage of the multi-sample measurements in comparison with BBM measurements is that the accuracy of the *ex-situ* data is higher. In addition to this, not only the transmittance data, but also the reflectance data and ellipsometric data are available. The multi-sample algorithm estimates the layer parameters on the basis of the minimization of the generalized DF GDF_{RT} [4,16,17]:

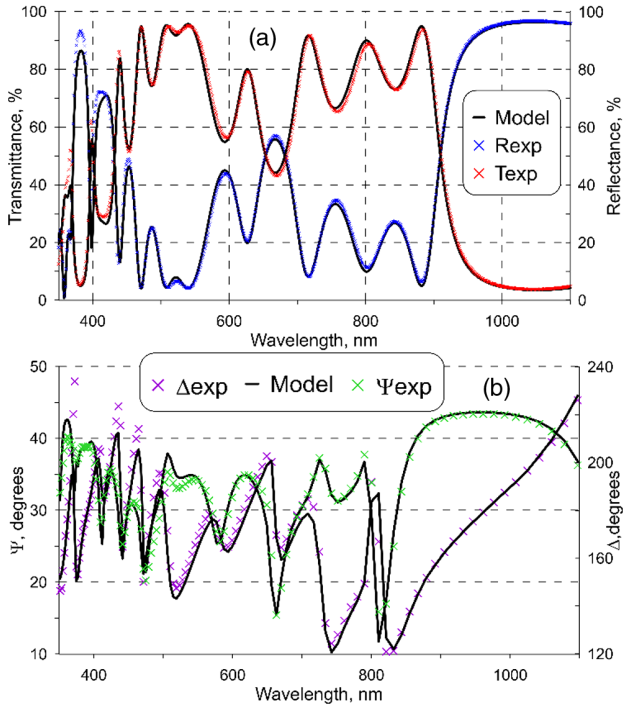

Fig. 7. Comparison of the experimental data related to the ML11 sample, and the model data calculated with the assumption that multilayer coating consists of layers with thicknesses and optical constants obtained during SL characterization: (a) spectral photometric data; (b) ellipsometric data, AOI = 45°.

$$\mathrm{GDF}_{\mathrm{RT}}^2 = \frac{1}{m}\sum_{i=1}^{m}\frac{1}{L}\sum_{j=1}^{L}\left[T(X^{(i)};\lambda_j) - \hat{T}(\lambda_j)\right]^2 + \left[R(X^{(i)};\lambda_j) - \hat{R}(\lambda_j)\right]^2. \quad (5)$$

In the case of ellipsometric measurements, Eq. (5) is rewritten as

$$\mathrm{GDF}_{\mathrm{ell}}^2 = \frac{1}{3m}\sum_{i=1}^{m}\sum_{q=1}^{3}\frac{1}{L}\sum_{j=1}^{L}\left[\frac{\Psi(X^{(i)};\theta_q;\lambda_j) - \hat{\Psi}^{(i)}(\lambda_j)}{\mu_j}\right]^2 + \left[\frac{\Delta\left(X^{(i)};\theta_q;\lambda_j\right) - \hat{\Delta}^{(i)}(\lambda_j)}{\nu_j}\right]^2 + \left[\frac{\xi(X^{(i)};\theta_q;\lambda_j) - \hat{\xi}^{(i)}(\lambda_j)}{\chi_j}\right]^2. \quad (6)$$

In Eqs. (5) and (6), the vector $X^{(i)}$ describes the i-layer coating the ML_i: $X^{(i)} = (d_1(1+\delta_1), \ldots, d_i(1+\delta_i), n_H + \varepsilon_1, n_L + \varepsilon, n_H + \varepsilon_3, \ldots, n_H + \varepsilon_i)$; where δ_i is the thickness relative error in the ith layer, and ε_i and ε are the refractive index offsets in the ith layer of the TiO_2 and SiO_2 layers, respectively. Compared with the DFs defined by Eqs. (2) and (3), the generalized DFs take the data related to all ML samples into account, not only the last one. The last vector $X^{(11)}$ was considered as the characterization result delivered by the multi-sample algorithm. As the SiO_2 layers are more stable, it was assumed that its offset ε is the same for all layers. The generalized DFs [Eqs. (5) and (6)] can be optimized with respect to the model vector X in different ways.

At the *first characterization attempt (briefly, $n-d$ algorithm)*, the GDF function was minimized in two steps: first, by the refractive index offsets ε_i, ε and, secondly, with respect to the relative errors δ_i. The results of this two-step algorithm are presented in Fig. 8. It is seen that the estimated thickness errors do not correspond to the errors determined during SL characterization. Additionally, the refractive index values take absolute non-realistic values. These observations are valid for both datasets: R/T and Ψ/Δ. Due to this comparison, it was stated that two-step optimization of GDF does not provide reliable values of the actual layer parameters. In addition, the thickness errors and refractive indices estimated from R/T and ellipsometry are not correlated.

At the *second characterization attempt (briefly, $d-n$ algorithm)*, the GDF function was minimized in two steps: first, by the relative errors δ_i and then by the refractive index offsets ε_i, ε. The results (Fig. 8) obtained in this way are in better correspondence with the parameters obtained during SL characterization.

At the *third characterization attempt (briefly, one-step algorithm)*, the GDF function was minimized simultaneously with respect to the relative errors δ_i as well as the refractive index offsets ε_i, ε. In Fig. 9, characterization results obtained by a one-step algorithm and SL characterization results are compared. One can observe a good correspondence between the determined layer parameters. Small deviations between the parameter values might have their origin in slightly different structures of the SL and ML samples, as mentioned before.

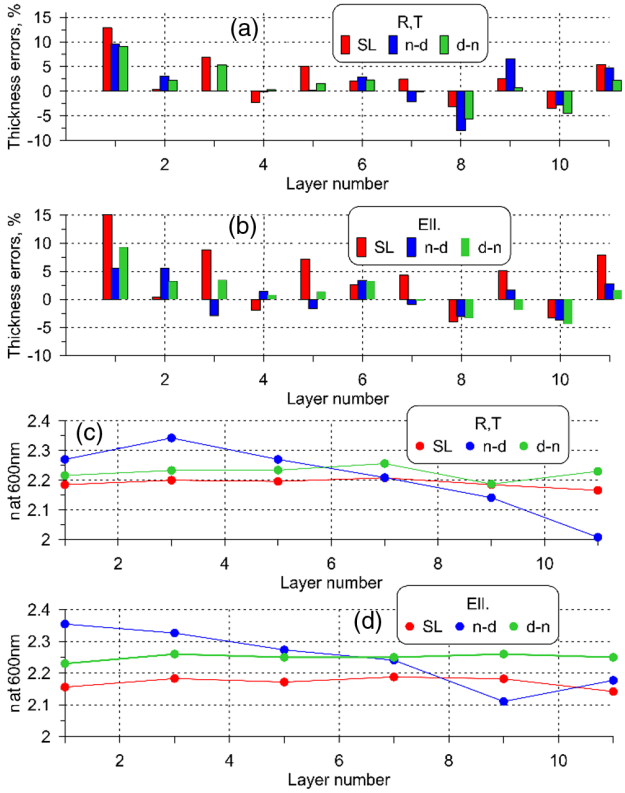

Fig. 8. Comparison of the relative errors in the (a), (b) layer thicknesses and (c), (d) refractive indices determined during the SL characterization and in the course of two-step $n-d$ and $d-n$ algorithms: (a), (c) R/T data and (b), (d) ellipsometric measurements.

5. SELECTION OF CHARACTERIZATION APPROACH FOR THE FINAL ML COATING BASED ON STANDARD *EX-SITU* MEASUREMENTS

It was shown in Section 4 that, in the case of e-beam deposited coatings, a one-step multi-sample algorithm provides reliable characterization results, similar to the results obtained from the single-layer samples.

Evidently, the proposed experiment is too complicated and time consuming to be carried out on a regular basis. At the same time, not all researchers are able to get *in-situ* measurements (for example, BBM measurements) and, as it had been mentioned in the Introduction, these measurements do not provide direct characterization of e-beam evaporated coatings. Typically, researchers try to extract the layer parameters from R/T or Ψ/Δ data related to a produced sample. However, it is quite easy to obtain unreliable results based on just a single measurement. Some examples of such reliable and unreliable characterization are presented in [7].

Having results obtained with the help of SL characterization and the multi-sample algorithm, it is possible to select an adequate coating model and a corresponding reliable numerical algorithm. Thus, results obtained from characterization of the

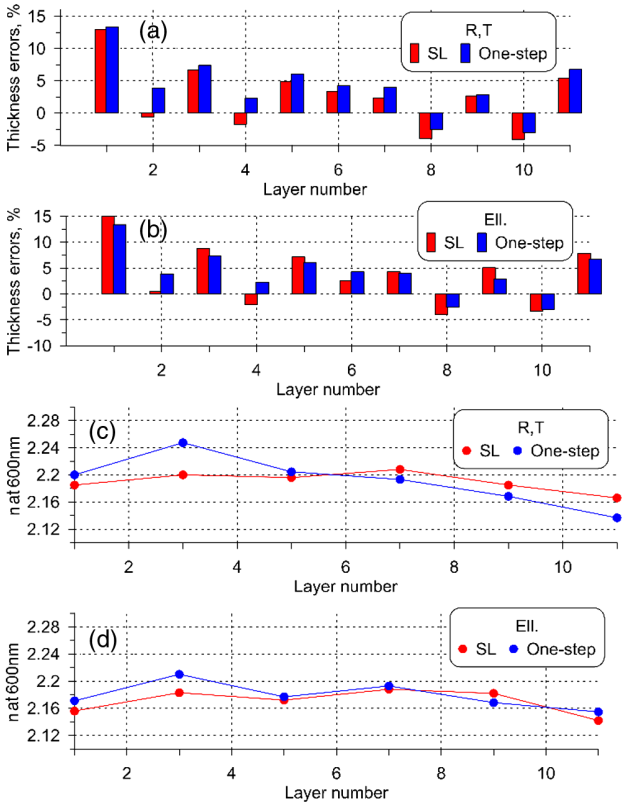

Fig. 9. Comparison of the relative errors in the (a), (b) layer thicknesses and (c), (d) refractive indices determined during the SL characterization process and during a one-step multi-sample algorithm based on the multi-sample data: (a), (c) R, T data and (b), (d) ellipsometric measurements.

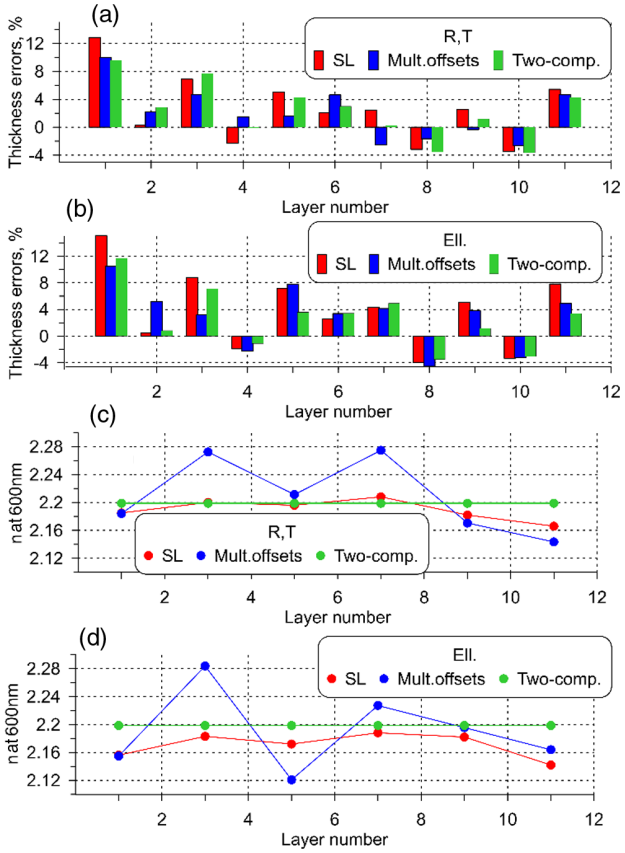

Fig. 10. Relative errors in the layer thicknesses and refractive indices determined from (a), (c) R, T and (b), (d) ellipsometric data related to the ML_{11} sample with the help of SL characterization, reverse engineering with multiple offsets, and reverse engineering with two offsets only.

experimental dataset already presented in this work are useful for the proper selection of the characterization approach, giving reliable results as well, but based on a single measurement of the final ML coating.

Typically, during a *standard reverse engineering (RE)* process, the layer parameters are being estimated based on minimization of the standard DF [Eq. (3) or (4)]. Based on the results of multi-sample characterization performed above, the DF should be minimized simultaneously with respect to the relative errors in the layer thicknesses δ_i and refractive index offsets ε_i, ε. First, it was assumed that all refractive index offsets may take different values, i.e., the set of the optimized parameters was the same as in the multi-sample one-step characterization algorithm (briefly, *RE, multiple offsets*). The layer parameters found during the application of this algorithm are shown in Figs. 10(a) and 10(b) by blue bars and in Figs. 10(c) and 10(d) by blue markers. It is seen that the correspondence between the thickness errors is good, but the refractive index values differ significantly from those obtained during SL characterization and estimated by the multi-sample algorithm, especially in the case of the ellipsometric data. This inconsistency can be explained by the fact that too many parameters (11 thicknesses $d_1, \ldots, d_{11}$ and 7 refractive index offsets $\varepsilon_1, \varepsilon_3, \ldots, \varepsilon_{11}, \varepsilon$; totally 18 parameters) were estimated on the basis of one spectrum only.

To simplify the model, it was assumed that all refractive index offsets ε_i take the same value (*briefly, RE, two-component*). In this case, a good fitting of experimental data by model data was achieved. The relative errors in the layer thicknesses are close to the ones obtained from SL characterization.

The reverse engineering results obtained with the help of the simplified model deliver not detailed but averaged results. Nevertheless, these results can be considered to be reliable, and they provide feedback to the deposition process.

In Table 1, the standard disc DF values and generalized discrepancies GDF are summarized. One can observe that all considered combinations, *coating model* and *algorithm*, provide discrepancies that are significantly lower than initial discrepancy. At the same time, only three of the combinations deliver reliable post-production characterization results: SL, multi-sample one-step, and RE two-component. This means that essential decrease of the DF cannot be considered as an indication of the reliability of characterization results. Moreover, there is no reason to state that one characterization approach is more reliable than another only because it provides lower values of the DF.

6. CONCLUSION

In the present work, a comprehensive study aimed at reliable characterization of e-beam deposited coatings was performed. In the course of the study, three questions formulated in the Introduction were answered.

- Reflectance and transmittance spectra and/or ellipsometric measurements related to the produced sample taken in a broadband range are a sufficient experimental dataset for reliable, but not detailed, results.
- Based on this data, only a simplified coating model can be applied. The model assumes the random errors in the layer thicknesses and the same offset in all layer refractive indices.
- The model does not provide detailed information about layer index variations. The numerical method is to be based on the simultaneous minimization of the DF with respect to the random errors in the layer thicknesses and refractive index offset.

The authors believe that the proposed approach will work perfectly with any types of coatings, which do not contain optically thin layers. Additionally, it would be interesting to study how this approach would manage with ultrathin layers. The ellipsometric data can be used as a sensitive and informative tool for such coatings.

Disclosures. The authors declare no conflicts of interest.

Data availability. Data underlying the results presented in this paper are not publicly available at this time but may be obtained from the authors upon reasonable request.

REFERENCES

1. T. Amotchkina, M. Trubetskov, A. Tikhonravov, I. B. Angelov, and V. Pervak, "Reliable optical characterization of e-beam evaporated TiO_2 films deposited at different substrate temperatures," Appl. Opt. **53**, A8–A15 (2014).
2. W. P. Thoeni, "Deposition of optical coatings: Process control and automation," Thin Solid Films **88**, 385–397 (1982).
3. L. Frey, P. Parrein, L. Virot, C. Pellé, and J. Raby, "Thin film characterization for modeling and optimization of silver-dielectric color filters," Appl. Opt. **53**, 1663–1673 (2014).
4. T. V. Amotchkina, M. K. Trubetskov, V. Pervak, S. Schlichting, H. Ehlers, D. Ristau, and A. V. Tikhonravov, "Comparison of algorithms used for optical characterization of multilayer optical coatings," Appl. Opt. **50**, 3389–3395 (2011).
5. D. Ristau, H. Ehlers, T. Gross, and M. Lappschies, "Optical broadband monitoring of conventional and ion processes," Appl. Opt. **45**, 1495–1501 (2006).
6. S. Wilbrandt, O. Stenzel, N. Kaiser, M. K. Trubetskov, and A. V. Tikhonravov, "In situ optical characterization and reengineering of interference coatings," Appl. Opt. **47**, C49–C54 (2007).
7. T. V. Amotchkina, M. K. Trubetskov, V. Pervak, B. Romanov, and A. V. Tikhonravov, "On the reliability of reverse engineering results," Appl. Opt. **51**, 5543–5551 (2012).
8. T. V. Amotchkina, M. K. Trubetskov, A. V. Tikhonravov, S. Schlichting, H. Ehlers, D. Ristau, D. Death, R. J. Francis, and V. Pervak, "Quality control of oblique incidence optical coatings based on normal incidence measurement data," Opt. Express **21**, 21508–21522 (2013).
9. A. V. Tikhonravov, T. V. Amotchkina, M. K. Trubetskov, R. J. Francis, V. Janicki, J. Sancho-Parramon, H. Zorc, and V. Pervak, "Optical characterization and reverse engineering based on multiangle spectroscopy," Appl. Opt. **51**, 245–254 (2012).
10. P. Baumeister, *Optical Coating Technology* (SPIE Optical Engineering, 2004).
11. Z. Czigány and G. Radnóczi, "Columnar growth structure and evolution of wavy interface morphology in amorphous multilayered thin films," Thin Solid Films **343–344**, 5–8 (1999).
12. M. K. Trubetskov and A. V. Tikhonravov, "OptiLayer software," http://www.optilayer.com.
13. O. Stenzel, S. Wilbrandt, N. Kaiser, M. Vinnichenko, F. Munnik, A. Kolitsch, A. Chuvilin, U. Kaiser, J. Ebert, S. Jakobs, A. Kaless, S. Wüthrich, O. Treichel, B. Wunderlich, M. Bitzer, and M. Grössl, "The correlation between mechanical stress, thermal shift and refractive index in HfO2, Nb2O5, Ta2O5 and SiO2 layers and its relation to the layer porosity," Thin Solid Films **517**, 6058–6068 (2009).
14. A. V. Tikhonravov, M. K. Trubetskov, A. V. Krasilnikova, E. Masetti, A. Duparré, E. Quesnel, and D. Ristau, "Investigation of the surface micro-roughness of fluoride films by spectroscopic ellipsometry," Thin Solid Films **397**, 229–237 (2001).
15. A. V. Tikhonravov, M. K. Trubetskov, T. V. Amotchkina, G. DeBell, V. Pervak, A. K. Sytchkova, M. L. Grilli, and D. Ristau, "Optical parameters of oxide films typically used in optical coating production," Appl. Opt. **50**, C75–C85 (2010).
16. O. Stenzel, *Optical Coatings*, Springer Series in Surface Sciences (Springer, 2014), Vol. **54**.
17. A. V. Tikhonravov and M. K. Trubetskov, "On-line characterization and reoptimization of optical coatings," Proc. SPIE **5250**, 406–413 (2004).